

EFFECTS OF VISCOUS DISSIPATION AND WALL CONDUCTION ON STEADY MIXED CONVECTION COUETTE FLOW OF HEAT GENERATING/ABSORBING FLUID

A.O. AJIBADE and A. M. UMAR*

Department of Mathematics, Ahmadu Bello University
Zaria, NIGERIA

E-mails: aoajibade@abu.edu.ng; amumar@abu.edu.ng

This article theoretically investigated mixed convection flow of heat generating/absorbing fluid in the presence of viscous dissipation and wall conduction effects. The flow is considered to be steady in a vertical channel with some boundary thickness. One of the plates is heated while the other is kept at ambient temperature. The governing flow equations were solved analytically using Homotopy Perturbation Method (HPM). The influences of the governing parameters were captured in graphs, tables and a table was constructed for validation of the work. It is worthwhile to stress that, both the velocity and temperature profiles decrease near the heated plate with an increase in boundary thickness (d) while the reverse cases were observed toward the cold plate. The velocity profile increases near the heated plate with increase in mixed convection parameter (Gre) and decreases towards the cold plate. Rate of heat transfer has been observed to decrease with increase in boundary plate thickness (d) while the critical value of (Gre) increases with growing boundary plate thickness. The study therefore established the importance of boundary plate thickness in mixed convection investigation.

Key words: mixed convection, viscous dissipation, vertical channel, boundary thickness, mass constant flux.

1. Introduction

Research in fluid dynamics receives great concern due to its application in science and engineering. The influences of fluid flow and thermophysical properties are investigated to suit industrial technology and sciences. Applications of fluid dynamics can be found in lubrication industries, cooling of electrical appliances, gas turbines, geothermal energy, cooling of nuclear reactors, plasma physics, gas drainage, petroleum industries, food processing industries etc.

In lubrication industries, viscous dissipation cannot be neglected since internal mechanical energy generated as a result of fluid particles' interaction affects the fluid flow and thermal behaviour in the system. Likewise, the boundary thickness and the thermal conductivity have effects on the fluid flow and heat flux. Kevin and Barbaros [1] investigated effect of axial conduction on heat transfer in a liquid flow. They concluded that, the amount of heat carried away from the heated region by wall is controlled by the wall thickness and the wall thermal conductivity. In the study of effects of wall heat conduction on the reforming process of methane in microreactor, Michael and Dimos [2] found that, heat transport through the solid wall is not only dependent on the thermal conductivity of the wall but also on the cross-sectional area of the solid. Hassab *et al.* [3] conducted a research on the effect of axial wall conduction on heat transfer for a parallel plate channel. Their result showed that, increase in wall thickness is interpreted as increasing thermal resistance to the heat transfer. Ates *et al.* [4] presented a paper on transient conjugated heat transfer in thick walled pipes with uniform heat flux boundary condition. They found that more heat penetrated backward through the upstream region by axial conduction in thick walled pipes, while in thin walled pipes, heat flux values are high. Mei *et al.* [5] examined the criteria of axial wall heat conduction under two classical thermal

* To whom correspondence should be addressed

boundary conditions. They showed that, the temperature gradient number for the thin-wall tube is higher than that for the thick-wall tube. The effect of wall conduction on mixed convection heat transfer in externally finned pipes was studied by Moukalled *et al.* [6]. They observed that, axial wall conduction in the pipe wall is found to strongly affect the flow and thermal fields and also buoyancy effects are stronger when the pipe wall conductivity is considered which increases the overall heat transfer to the fluid.

Hamid and Behnam [7], Ajibade and Thomas [8] and Swati [9] reported that both velocity and temperature profiles increase with increase in mixed convection Gre . Jha *et al.* [10] investigated mixed convection in an inclined channel filled with porous material. They observed that, the flow is reversal type, the tendency of reversal has increasing trend with increasing positive mixed convection on the lower inclined channel wall whereas the trend increased with increasing negative mixed convection on the sinusoidally hot wall. Mehdi and Mohsen [11] examined mixed convection slip flow in a vertical parallel plate with asymmetric and uniform heat flux. Their result showed that, for a higher value of mixed convection parameter values, the slip velocity increases on the hot wall and drops on the cold wall for heat flux ratio (rq). Jha *et al.* [12] investigated a steady fully developed mixed convection flow in a vertical parallel plate with bilateral heating and the microchannel is filled with porous material. They found that, increasing mixed convection parameter Gre leads to decrease in fluid flow near the cold wall, whereas near the hot wall, increasing Gre leads to an increase in velocity. They also concluded that, the fluid flow is not affected by the Gre at the middle of the channel. An exact solution of steady fully developed mixed convection flow in a vertical micro-porous-annulus was studied by Jha and Babatunde [13]. They concluded that, near the outer surface of the inner porous cylinder, increasing GR leads to decrease in fluid velocity whereas near the inner surface of the outer porous cylinder, increasing Gr leads to an increase in fluid velocity.

Dileep and Vikas [14] studied radiation effects on mixed convection flow and viscous heating in a vertical channel partially filled with porous medium. They indicated that, temperature increases due to viscous dissipation effects in the channel. Joseph *et al.* [15] examined effect of Brinkman number and magnetic field on Laminar flow in a vertical plate channel. They found that, Brinkman number has accelerating effect on the temperature. Viscous dissipation effects on the limiting value of Nusselt numbers for a shear driven flow between two asymmetrically heated parallel plates was investigated by Pranab and Sanchayan [16]. They showed that, a strong influence of viscous dissipation is quite significant for analysis of heat transfer in the conduction limit.

Jha and Ajibade [17] studied unsteady free convection Couette flow of heat generating/absorbing fluid where they discovered that, the fluid temperature is the same as that of the isothermal moving plate and thus there is no heat transfer between the fluid and the plate at the steady state. The work of Jha *et al.* [18] recently investigated steady fully developed mixed convection flow in a vertical channel with heat generation/absorption effect. They discovered that, the temperature profile increases with increase in heat generation parameter while a reverse trend occurs in the case of heat absorption parameter. Heat generation/absorption is considered as a linear function of local temperature in some articles. Vajravelu and Sastri [19-20] investigated Laminar free convection heat transfer of a viscous incompressible heat generating fluid flow past a vertical porous plate in the presence of free-stream oscillations. Part I of the article deals with the mean flow and heat transfer and part II deals with the unsteady flow and heat transfer. Also Vajravelu [21] in his work studied natural convection at a heated vertical plate with temperature dependent heat sources/sinks. Moalem [22] considered temperature dependent heat source of the type $Q' \alpha \frac{I}{(a+bT)}$ on

the steady state heat transfer within a porous medium. Foraboschi and Federico [23] considered volumetric rate of heat generation of the type $Q = Q_0(T - T_0)$ when $T \geq T_0$. Therefore, due to the temperature difference which is directly proportional to channel walls, this work adopts the work of Foraboschi and Federico [23].

None of the reviewed works above carried out a study on the viscous dissipation and wall conduction effects on steady mixed convection flow of heat generating/absorbing fluid in a vertical channel. Due to the application of viscous dissipation, wall conductivity, boundary thickness and mixed convection in lubrication industries, cooling of nuclear reactors, cooling of electric appliances etc. It is pertinent to investigate how

temperature, velocity, wall conduction and energy generated can be controlled in a vertical channel by these governing thermophysical and flow parameters, hence the present article.

The momentum and energy equations in the present model are coupled and nonlinear and as such, obtaining a closed form solution is a daunting task. Various solutions methods have been derived for such problems and this ranges from numerical solutions, perturbation methods and several other approximate solutions techniques, this problem has adopted the homotopy perturbation technique as the solution method.

2. Mathematical analysis

A two-dimensional steady flow of an incompressible viscous fluid passes through vertical parallel plates is considered (see Fig.1). The plate p_1 is heated while p_2 is kept at ambient temperature with thickness d^* . The fluid and energy flow in the channel is subjected to mixed convection and wall conduction in the presence of viscous dissipation. The flow is assumed to be along x^* direction and y^* is normal to the plates. Internal energy is generated as a result of fluid particles interaction and the thermophysical properties are assumed to be constant of the linear momentum equation as approximated by Boussinesq approximation. It is assumed that, the physical equations that describe the situation following the work of Jha and Ajibade [17] taking into account: viscous dissipation, boundary thickness, pressure gradient and wall conduction effects are given as

$$\nu \frac{d^2 u^*}{dy^{*2}} + g\beta(T_f^* - T_0) - \frac{1}{\rho} \frac{dP^*}{dx^*} = 0, \quad (2.1)$$

$$\alpha_1 \frac{d^2 T_{p1}^*}{dy^{*2}} = 0, \quad (2.2)$$

$$\frac{k}{\rho c_p} \frac{d^2 T_f^*}{dy^{*2}} - \frac{Q_0}{c_p} (T_f^* - T_0) + \frac{\nu}{c_p} \left(\frac{du^*}{dy^*} \right)^2 = 0, \quad (2.3)$$

$$\alpha_2 \frac{d^2 T_{p2}^*}{dy^{*2}} = 0 \quad (2.4)$$

where y^* and x^* are the dimensional distances along and perpendicular to the plate. u^* and T_f^* are the dimensional fluid velocity and fluid temperature. Q_0 , ν , k , ρ , c_p , β and g are the dimensional heat source/sink coefficient, kinematic viscosity, thermal conductivity, density, specific heat at constant pressure, thermal expansion coefficient and acceleration due to gravity of the fluid respectively. α_1 and α_2 are the thermal diffusivity of p_1 and p_2 respectively. P^* is the dimensional pressure gradient. The first, second and third term of Eq.(2.1) are the viscosity, thermal buoyancy and pressure gradient effects on the fluid. Also the first, second and third term of Eq.(2.3) are thermal conductivity, heat source/sink, and viscous dissipation effect of the fluid.

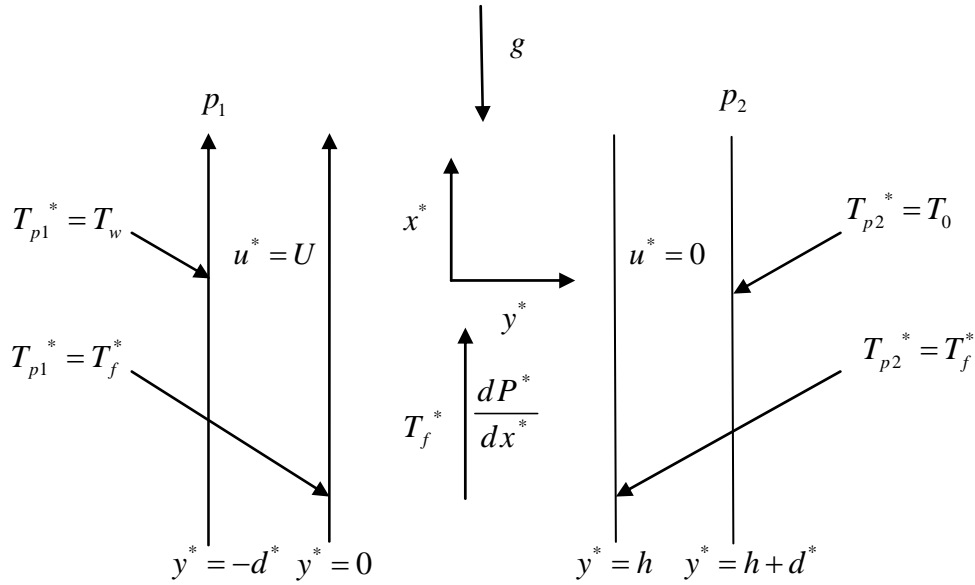


Fig.1. Schematic diagram of the problem.

To maintain the steady state flow, we assume that the appropriate boundary conditions of the model are

$$\begin{aligned}
 u^* &= U & \text{at} & \quad y^* = 0, \\
 u^* &= 0 & \text{at} & \quad y^* = h, \\
 T_{p1}^* &= T_w & \text{at} & \quad y^* = -d^*, \\
 T_{p1}^* &= T_f^* & \text{at} & \quad y^* = 0, \\
 k_1 \frac{dT_{p1}^*}{dy^*} &= k \frac{dT_f^*}{dy^*} & \text{at} & \quad y^* = 0, \\
 T_{p2}^* &= T_f^* & \text{at} & \quad y^* = h, \\
 k_2 \frac{dT_{p2}^*}{dy^*} &= k \frac{dT_f^*}{dy^*} & \text{at} & \quad y^* = h, \\
 T_{p2}^* &= 0 & \text{at} & \quad y^* = h + d^*.
 \end{aligned} \tag{2.5}$$

The temperature and flux conditions at $y^* = 0$ and $y^* = h$ are the inter-facial temperature and flux conditions respectively. U , T_w and T_0 are the velocity of the moving plate, temperature of the heated and

cold plate respectively. k_1 and k_2 are the thermal conductivities of p_1 and p_2 respectively. Below are the dimensionless quantities used

$$u = \frac{u^*}{U}, \quad y = \frac{y^*}{h}, \quad T_f = \frac{T_f^* - T_0}{T_w - T_0}, \quad T_{p1} = \frac{T_{p1}^* - T_0}{T_w - T_0}, \quad (2.6)$$

$$T_{p2} = \frac{T_{p2}^* - T_0}{T_w - T_0}, \quad d = \frac{d^*}{h}, \quad x = \frac{x^* v}{Uh^2}, \quad P = \frac{P^*}{\rho U^2}.$$

Using the dimensionless quantities (2.6) above, the momentum and energy Eqs (2.1)-(2.4) are presented as

$$\frac{d^2 u}{dy^2} + Gre T_f - \frac{dP}{dx} = 0, \quad (2.7)$$

$$\frac{d^2 T_{p1}}{dy^2} = 0, \quad (2.8)$$

$$\frac{d^2 T_f}{dy^2} + Br \left(\frac{du}{dy} \right)^2 - ST_f = 0, \quad (2.9)$$

$$\frac{d^2 T_{p2}}{dy^2} = 0, \quad (2.10)$$

and the boundary conditions are

$$\begin{aligned} u &= 1 && \text{at } y = 0, \\ u &= 0 && \text{at } y = 1, \\ T_{p1} &= 1 && \text{at } y = -d, \\ T_{p1} &= T_f && \text{at } y = 0, \\ \frac{dT_{p1}}{dy} &= kr_1 \frac{dT_f}{dy} && \text{at } y = 0, \\ T_{p2} &= T_f && \text{at } y = 1, \\ \frac{dT_{p2}}{dy} &= kr_2 \frac{dT_f}{dy} && \text{at } y = 1, \\ T_{p2} &= 0 && \text{at } y = 1 + d \end{aligned} \quad (2.11)$$

where Gre is the mixed convection parameter, Pr is the Prandtl number, Ec is Eckert number, S is heat generation/absorption parameter, $EcPr = Br$ Brinkman number. kr_1 and kr_2 are the thermal conductivity ratios of the bounding slabs p_1 and p_2 .

$$Gre = \frac{Gr}{Re} = \frac{g\beta(T_w - T_0)h^3}{\nu^2} \cdot \frac{\nu}{Uh}, \quad Pr = \frac{\nu}{\alpha}, \quad S = \frac{Q_0 h^2}{k},$$

$$Ec = \frac{U^2}{c_p(T_w - T_0)}, \quad EcPr = Br, \quad kr_1 = kr_2 = \frac{k}{k_1} = \frac{k}{k_2} = 1.$$

3. Method of solution

There are so many analytical and numerical methods to find the approximate solution of nonlinear differential equations. Such methods are: Homotopy Analysis Method (HAM), Adomian Decomposition Method (ADM), Differential Transform Method (DTM), Finite Difference Method (FDM), Finite Element Method (FEM), Runge Kutta Method etc. Homotopy Perturbation Method (HPM) is chosen in this work because the method requires no small parameters in equations and can readily eliminate the limitation of traditional perturbation techniques. The method is also simple and furthermore, the first order approximations are of extreme accuracy than the second order of traditional perturbation. The method converges as shown by Jafar and Hossein [24], Asma *et al.* [25], Elsayed *et al.* [26] and Jafar *et al.* [27]. The method was first initiated by He [28] to solve linear, nonlinear and coupled problems in partial or ordinary form. He [29], He [30] and He [31] also used the new method to solve nonlinear and boundary value problems. He [28] presented the method by considering the nonlinear differential equation

$$A(u) - f(r) = 0, \quad r \in \Omega.$$

With the boundary condition

$$B\left(u, \frac{\partial u}{\partial \eta}\right) = 0, \quad r \in \Gamma$$

where A is the general differential operator, B is a boundary operator, $f(r)$ is a known analytic function, Γ is the boundary of the domain Ω . The operator A can be divided into two parts, that is, L and N , where L is linear and N nonlinear parts. Therefore the nonlinear differential equation can be presented as

$$L(u) + N(u) - f(r) = 0.$$

Convex Homotopy can be constructed from the nonlinear differential equation and its boundary condition as

$$v(r, p): \Omega \times [0, 1] \rightarrow \Re \text{ which satisfies,}$$

$$H(v, p) = (1-p)[L(v) - L(u_0)] + p[A(v) - f(r)] = 0$$

or

$$H(v, p) = L(v) - L(u_0) + pL(u_0) + p[N(v) - f(r)] = 0$$

where $p \in [0, 1]$ is an embedding parameter, u_0 is the initial approximation of the nonlinear differential equation. which satisfies the boundary conditions. Therefore

$$H(v, 0) = L(v) - L(u_0) = 0, \quad (3.1)$$

$$H(v, 1) = A(v) - f(r) = 0.$$

Now the solution of the nonlinear differential equation is expressed as

$$v = v_0 + pv_1 + p^2v_2 + p^3v_3 + \dots$$

By setting $p = 1$, the approximate solution can be written as

$$v = v_0 + v_1 + v_2 + v_3 + \dots$$

Now the convex Homotopy of the momentum and energy equations are constructed as

$$H(u, p) = (1-p) \left[\frac{d^2u}{dy^2} - \frac{d^2v_0}{dy^2} \right] + p \left[\frac{d^2u}{dy^2} + GreT_f - \frac{dP}{dx} \right] = 0. \quad (3.2)$$

Since the zeroth order is linear and can be solved directly, then there is no need of initial approximation v_0 , therefore

$$\frac{d^2u}{dy^2} = p \left[\frac{dP}{dx} - GreT_f \right]. \quad (3.3)$$

Such that

$$u = u_0 + pu_1 + p^2u_2 + p^3u_3 + \dots$$

$$T_f = T_{f_0} + pT_{f_1} + p^2T_{f_2} + p^3T_{f_3} + \dots$$

(3.4)

$$T_{p_1} = T_{p_{10}} + pT_{p_{11}} + p^2T_{p_{12}} + p^3T_{p_{13}} + \dots$$

$$T_{p_2} = T_{p_{20}} + pT_{p_{21}} + p^2T_{p_{22}} + p^3T_{p_{23}} + \dots$$

Substituting Eqs (3.4) into Eq.(3.3), we have

$$\frac{d^2u_0}{dy^2} + p \frac{d^2u_1}{dy^2} + p^2 \frac{d^2u_2}{dy^2} + p^3 \frac{d^2u_3}{dy^2} + \dots = p \frac{dP}{dy} - pGreT_{f_0} - p^2GreT_{f_1} - p^3GreT_{f_2} + \dots (3.5)$$

Comparing the coefficient of $p^0, p^1, p^2, p^3, \dots$

$$p^0 : \frac{d^2 u_0}{dy^2} = 0, \quad (3.6)$$

$$p^1 : \frac{d^2 u_1}{dy^2} = \frac{dP}{dx} - GreT_{f_0}, \quad (3.7)$$

$$p^2 : \frac{d^2 u_2}{dy^2} = -GreT_{f_1}, \quad (3.8)$$

$$p^3 : \frac{d^2 u_3}{dy^2} = -GreT_{f_2}, \quad (3.9)$$

$$p^4 : \frac{d^2 u_4}{dy^2} = -GreT_{f_4}. \quad (3.10)$$

·
·
·

Similarly, since no initial approximation for Eqs (2.8), (2.9) and (2.10) also, then they are transformed as

$$p^0 : \frac{d^2 T_{p1_0}}{dy^2} = 0, \quad (3.11)$$

$$p^1 : \frac{d^2 T_{p1_1}}{dy^2} = 0, \quad (3.12)$$

$$p^2 : \frac{d^2 T_{p1_2}}{dy^2} = 0, \quad (3.13)$$

$$p^3 : \frac{d^2 T_{p1_3}}{dy^2} = 0, \quad (3.14)$$

$$p^4 : \frac{d^2 T_{p1_4}}{dy^2} = 0, \quad (3.15)$$

·
·
·

Eq.(2.9) is transformed as

$$\frac{d^2 T_f}{dy^2} = p \left[ST_f - \text{Br} \left(\frac{du}{dy} \right)^2 \right], \quad (3.16)$$

$$\begin{aligned} \frac{d^2 T_{f_0}}{dy^2} + p \frac{d^2 T_{f_1}}{dy^2} + p^2 \frac{d^2 T_{f_2}}{dy^2} + p^3 \frac{d^2 T_{f_3}}{dy^2} + \dots = p ST_{f_0} + p^2 ST_{f_1} + p^3 ST_{f_2} + \dots \\ - p \text{Br} \left(\frac{du_0}{dy} \right)^2 - p^2 2 \text{Br} \frac{du_0}{dy} \cdot \frac{du_1}{dy} - p^3 \left[2 \text{Br} \frac{du_0}{dy} \cdot \frac{du_2}{dy} + \text{Br} \left(\frac{du_1}{dy} \right)^2 \right] + \\ - p^4 \left[2 \text{Br} \frac{du_0}{dy} \cdot \frac{du_3}{dy} + 2 \text{Br} \frac{du_1}{dy} \cdot \frac{du_2}{dy} \right] + \dots \end{aligned} \quad (3.17)$$

Comparing the coefficient of $p^0, p^1, p^2, p^3, \dots$

$$p^0 : \frac{d^2 T_{f_0}}{dy^2} = 0, \quad (3.18)$$

$$p^1 : \frac{d^2 T_{f_1}}{dy^2} = ST_{f_0} - \text{Br} \left(\frac{du_0}{dy} \right)^2, \quad (3.19)$$

$$p^2 : \frac{d^2 T_{f_2}}{dy^2} = ST_{f_1} - 2 \text{Br} \frac{du_0}{dy} \cdot \frac{du_1}{dy}, \quad (3.20)$$

$$p^3 : \frac{d^2 T_{f_3}}{dy^2} = ST_{f_2} - 2 \text{Br} \frac{du_0}{dy} \cdot \frac{du_2}{dy} - \text{Br} \left(\frac{du_1}{dy} \right)^2, \quad (3.21)$$

⋮
⋮
⋮

and Eq.(2.10) is transformed as

$$p^0 : \frac{d^2 T_{p2_0}}{dy^2} = 0, \quad (3.22)$$

$$p^1 : \frac{d^2 T_{p2_1}}{dy^2} = 0, \quad (3.23)$$

$$p^2 : \frac{d^2 T_{p2_2}}{dy^2} = 0, \quad (3.24)$$

$$p^3 : \frac{d^2 T_{p23}}{dy^2} = 0, \quad (3.25)$$

$$p^4 : \frac{d^2 T_{p24}}{dy^2} = 0, \quad (3.26)$$

⋮
⋮
⋮

The boundary conditions are transformed as

$$u_0(0) = 1, \quad u_1(0) = u_2(0) = u_3(0) = \dots = 0,$$

$$u_0(1) = u_1(1) = u_2(1) = u_3(1) = \dots = 0,$$

$$T_{p10}(-d) = 1, \quad T_{p11}(-d) = T_{p12}(-d) = T_{p13}(-d) = \dots = 0,$$

$$T_{p10}(0) = T_{f0}, \quad T_{p11}(0) = T_{f1}, \quad T_{p12}(0) = T_{f2}, \quad T_{p13}(0) = T_{f3}, \dots,$$

$$\left. \frac{dT_{p10}}{dy} \right|_{y=0} = \frac{dT_{f0}}{dy}, \quad \left. \frac{dT_{p11}}{dy} \right|_{y=0} = \frac{dT_{f1}}{dy}, \quad \left. \frac{dT_{p12}}{dy} \right|_{y=0} = \frac{dT_{f2}}{dy}, \quad \left. \frac{dT_{p13}}{dy} \right|_{y=0} = \frac{dT_{f3}}{dy}, \dots, \quad (3.27)$$

$$T_{p20}(1) = T_{f0}, \quad T_{p21}(1) = T_{f1}, \quad T_{p22}(1) = T_{f2}, \quad T_{p23}(1) = T_{f3}, \dots,$$

$$\left. \frac{dT_{p20}}{dy} \right|_{y=1} = \frac{dT_{f0}}{dy}, \quad \left. \frac{dT_{p21}}{dy} \right|_{y=1} = \frac{dT_{f1}}{dy}, \quad \left. \frac{dT_{p22}}{dy} \right|_{y=1} = \frac{dT_{f2}}{dy}, \quad \left. \frac{dT_{p23}}{dy} \right|_{y=1} = \frac{dT_{f3}}{dy}, \dots,$$

$$T_{p20}(1+d) = T_{p21}(1+d) = T_{p22}(1+d) = T_{p23}(1+d) = \dots = 0.$$

Solving from above Eqs (3.6), (3.11), (3.18) and (3.22) and applying the boundary conditions (3.27)

$$u_0 = A_0 y + A_1, \quad (3.28)$$

$$T_{p10} = A_2 y + A_3, \quad (3.29)$$

$$T_{f0} = A_4 y + A_5, \quad (3.30)$$

$$T_{p20} = A_6 y + A_7, \quad (3.31)$$

$$A_0 = -1, \quad A_1 = 1, \quad A_2 = A_4 = A_6 = -\frac{1}{(1+2d)}, \quad A_3 = A_5 = A_7 = 1 + A_2 d.$$

Solving Eqs (3.7), (3.12), (3.19) and (3.23)

$$u_1 = \frac{y^2}{2} \frac{dP}{dx} - Gre \left[A_4 \frac{y^3}{6} + A_5 \frac{y^2}{2} \right] + A_8 y + A_9, \quad (3.32)$$

$$T_{p11} = A_{10} y + A_{11}, \quad (3.33)$$

$$T_{f1} = S \left[A_4 \frac{y^3}{6} + A_5 \frac{y^2}{2} \right] - Br \frac{y^2}{2} + A_{12} y + A_{13}, \quad (3.34)$$

$$T_{p21} = A_{14} y + A_{15}. \quad (3.35)$$

Applying the boundary conditions (3.27)

$$A_9 = 0, \quad A_8 = Gre \left[\frac{A_4}{6} + \frac{A_5}{2} \right] - \frac{1}{2} \frac{dP}{dx},$$

$$A_{12} = \frac{Br(1+d)}{(1+2d)} - \frac{Br}{2(1+2d)} + \frac{S}{(1+2d)} \left[\frac{A_4}{3} + \frac{A_5}{2} \right] - \frac{S(1+d)}{(1+2d)} \left[\frac{A_4}{2} + A_5 \right], \quad A_{13} = A_{12} d.$$

Solving Eqs (3.8), (3.13), (3.20) and (3.24), and applying the boundary conditions (3.27)

$$u_2 = -GreS \left[A_4 \frac{y^5}{120} + A_5 \frac{y^4}{24} \right] + Br Gre \frac{y^4}{24} - A_{12} Gre \frac{y^3}{6} - A_{13} Gre \frac{y^2}{2} + A_{16} y + A_{17}, \quad (3.36)$$

$$T_{p12} = A_{18} y + A_{19}, \quad (3.37)$$

$$T_{f2} = S^2 \left[A_4 \frac{y^5}{120} + A_5 \frac{y^4}{24} \right] - Br S \frac{y^4}{24} + A_{12} S \frac{y^3}{6} + A_{13} S \frac{y^2}{2} + Br \frac{y^3}{3} \frac{dP}{dx} - Gre Br \left[A_4 \frac{y^4}{12} + A_5 \frac{y^3}{3} \right] + Br A_8 y^2 + A_{20} y + A_{21}, \quad (3.38)$$

$$T_{p22} = A_{22} y + A_{23} \quad (3.39)$$

where

$$A_{17} = 0, \quad A_{16} = GreS \left[\frac{A_4}{120} + \frac{A_5}{24} \right] - \frac{Gre Br}{24} + \frac{A_{12} Gre}{6} + \frac{A_{13} Gre}{2},$$

$$A_{20} = \frac{BrS(1+d)}{6(1+2d)} - \frac{S^2(1+d)}{(1+2d)} \left[\frac{A_4}{24} + \frac{A_5}{6} \right] - \frac{A_{12}S(1+d)}{2(1+2d)} - \frac{A_{13}S(1+d)}{(1+2d)} - \frac{Br(1+d)}{(1+2d)} \frac{dP}{dx} + \frac{Gre Br(1+d)}{(1+2d)} \left[\frac{A_4}{3} + A_5 \right] - \frac{2Br A_8(1+d)}{(1+2d)} - \frac{BrS}{8(1+2d)} - \frac{S^2}{(1+2d)} \left[\frac{A_4}{30} + \frac{A_5}{8} \right] + \frac{A_{12}S}{3(1+2d)} + \frac{A_{13}S}{2(1+2d)} + \frac{2Br}{3(1+2d)} \frac{dP}{dx} - \frac{Gre Br}{(1+2d)} \left[\frac{A_4}{4} + \frac{2A_5}{3} \right] + \frac{A_8 Br}{(1+2d)},$$

$$A_{21} = A_{20}d.$$

Solving Eqs (3.9), (3.14), (3.21) and (3.25)

$$\begin{aligned} u_3 = & -GreS^2 \left[A_4 \frac{y^7}{5040} + A_5 \frac{y^6}{720} \right] + Br GreS \frac{y^6}{720} - A_{12} GreS \frac{y^5}{120} + \\ & -A_{13} GreS \frac{y^4}{24} + Gre Br \frac{y^5}{60} \frac{dP}{dx} + Gre^2 Br \left[A_4 \frac{y^6}{360} + A_5 \frac{y^5}{60} \right] + \\ & -GreA_8 Br \frac{y^4}{12} - GreA_{20} \frac{y^3}{6} - GreA_{21} \frac{y^2}{2} + A_{24}y + A_{25}, \end{aligned} \quad (3.40)$$

$$T_{p13} = A_{26}y + A_{27}, \quad (3.41)$$

$$\begin{aligned} T_{f2} = & S^3 \left[A_4 \frac{y^7}{5040} + A_5 \frac{y^6}{720} \right] - Br S^2 \frac{y^6}{720} + A_{12} S^2 \frac{y^5}{120} + A_{13} S^2 \frac{y^4}{24} + \\ & + Br S \frac{y^5}{60} \frac{dP}{dx} + A_8 Br S \frac{y^2}{12} + A_{20} S \frac{y^3}{6} + A_{21} S \frac{y^2}{2} - Gre Br S \left[A_4 \frac{y^6}{180} + A_5 \frac{y^5}{30} \right] + \\ & + Br^2 Gre \frac{y^5}{60} - A_{12} Gre Br \frac{y^4}{12} - A_{13} Gre Br \frac{y^3}{3} + A_{16} Br y^2 - Br \left(\frac{dP}{dx} \right)^2 \frac{y^4}{12} + \\ & + Gre Br \frac{dP}{dx} \left[A_4 \frac{y^5}{20} + A_5 \frac{y^4}{6} \right] - A_8 Br \frac{dP}{dx} \frac{y^3}{3} - Gre^2 Br \left[A_4^2 \frac{y^6}{120} + A_4 A_5 \frac{y^5}{20} + A_5^2 \frac{y^4}{12} \right] + \\ & + Gre Br A_8 \left[A_4 \frac{y^4}{12} + A_5 \frac{y^3}{3} \right] - Br A_8^2 \frac{y^2}{2} + A_{28}y + A_{29}, \end{aligned} \quad (3.42)$$

$$T_{p23} = A_{30}y + A_{31}. \quad (3.43)$$

Applying the boundary conditions (3.27)

$$A_{25} = 0,$$

$$\begin{aligned} A_{24} = & GreS^2 \left[\frac{A_4}{5040} + \frac{A_5}{720} \right] - \frac{Gre Br S}{720} + \frac{A_{12} Gre S}{120} + \frac{A_{13} Gre S}{24} + \\ & - Gre^2 Br \left[\frac{A_4}{360} + \frac{A_5}{60} \right] + \frac{A_8 Gre Br}{12} + \frac{A_{20} Gre}{6} + \frac{A_{21} Gre}{2}, \end{aligned}$$

$$\begin{aligned}
A_{28} = & \frac{BrS^2(1+d)}{120(1+2d)} - \frac{S^3(1+d)}{(1+2d)} \left[\frac{A_4}{720} + \frac{A_5}{120} \right] - \frac{A_{12}S^2(1+d)}{24(1+2d)} + \\
& - \frac{A_{13}S^2(1+d)}{6(1+2d)} - \frac{BrS(1+d)}{12(1+2d)} \frac{dP}{dx} + \frac{GreBrS(1+d)}{(1+2d)} \left[\frac{A_4}{30} + \frac{A_5}{6} \right] + \\
& - \frac{BrA_8S(1+d)}{3(1+2d)} - \frac{A_{20}S(1+d)}{2(1+2d)} - \frac{A_{21}S(1+d)}{(1+2d)} - \frac{Br^2Gre(1+d)}{12(1+2d)} + \\
& + \frac{A_{12}BrGre(1+d)}{3(1+2d)} + \frac{A_{13}BrGre(1+d)}{(1+2d)} - \frac{2A_{16}Br(1+d)}{(1+2d)} + \frac{Br(1+d)}{3(1+2d)} \left(\frac{dP}{dx} \right)^2 + \\
& - \frac{BrGre(1+d)}{(1+2d)} \frac{dP}{dx} \left[\frac{A_4}{4} + \frac{2A_5}{3} \right] + \frac{A_8Br(1+d)}{(1+2d)} \frac{dP}{dx} + \frac{BrGre^2(1+d)}{(1+2d)} \left[\frac{A_4^2}{20} + \frac{A_4A_5}{4} + \frac{A_5^2}{3} \right] + \\
& - \frac{GreBrA_8}{(1+2d)} \left[\frac{A_4}{3} + A_5 \right] + \frac{BrA_8^2(1+d)}{(1+2d)} + \frac{S^3}{(1+2d)} \left[\frac{A_4}{840} + \frac{A_5}{144} \right] - \frac{BrS^2}{144(1+2d)} + \frac{A_{12}S^2}{30(1+2d)} + \\
& + \frac{A_{13}S^2}{8(1+2d)} + \frac{BrS}{15(1+2d)} \frac{dP}{dx} - \frac{GreBrS}{(1+2d)} \left[\frac{A_4}{36} + \frac{2A_5}{15} \right] + \frac{A_8BrS}{4(1+2d)} + \frac{A_{20}S}{3(1+2d)} + \frac{A_{21}S}{2(1+2d)} + \\
& + \frac{Br^2Gre}{15(1+2d)} - \frac{A_{12}GreBr}{4(1+2d)} - \frac{2A_{13}GreBr}{3(1+2d)} + \frac{A_{16}Br}{(1+2d)} - \frac{Br}{4(1+2d)} \left(\frac{dP}{dx} \right)^2 + \\
& + \frac{GreBr}{(1+2d)} \frac{dP}{dx} \left[\frac{A_4}{5} + \frac{A_5}{2} \right] - \frac{2A_8Br}{3(1+2d)} \frac{dP}{dx} - \frac{Gre^2Br}{(1+2d)} \left[\frac{A_4^2}{24} + \frac{A_4A_5}{5} + \frac{A_5^2}{4} \right] + \\
& + \frac{GreBrA_8}{(1+2d)} \left[\frac{A_4}{4} + \frac{2A_5}{3} \right] - \frac{BrA_8^2}{2(1+2d)},
\end{aligned}$$

$$A_{29} = A_{28}d.$$

Therefore, the approximate solution of momentum and energy Eqs (2.7) and (2.9) as $p \rightarrow 1$ are

$$u = u_0 + u_1 + u_2 + u_3 + \dots, \quad (3.44)$$

$$T_f = T_{f_0} + T_{f_1} + T_{f_2} + T_{f_3} + \dots \quad (3.45)$$

The physical quantities of interest are the shear stress, rate of heat transfer, reverse flow and pressure gradient of the fluid.

To obtain the pressure gradient required to derive this flow for a constant mass flux q the integral

$$\int_0^1 u dy = q, \quad (3.46)$$

is evaluated so as to obtain the pressure gradient for varying value of q . The pressure gradient can be expressed as

$$\frac{dP}{dx} = \frac{A}{B} \quad (3.47)$$

where

$$\begin{aligned}
A = & \frac{1}{2} + Gre \left[\frac{A_4}{24} + \frac{A_5}{12} \right] + GreS \left[\frac{A_4}{360} + \frac{A_5}{80} \right] - \frac{Gre Br}{80} + \frac{A_{12}Gre}{24} + \frac{A_{13}Gre}{12} + \\
& + GreS^2 \left[\frac{A_4}{13440} + \frac{A_5}{2016} \right] - \frac{Gre Br S}{2016} + \frac{A_{12}GreS}{360} + \frac{A_{13}GreS}{80} + Gre^2 Br \left[\frac{A_4}{315} + \frac{A_5}{144} \right] + \\
& + \frac{Gre Br S (1+d)}{14(1+2d)} - \frac{GreS^2 (1+d)}{24(1+2d)} \left[\frac{A_4}{24} + \frac{A_5}{12} \right] - \frac{GreA_{12}S (1+d)}{48(1+2d)} - \frac{GreA_{13}S (1+d)}{24(1+2d)} + \\
& - \frac{Gre Br S}{192(1+2d)} - \frac{GreS^2 (1+d)}{24(1+2d)} \left[\frac{A_4}{30} + \frac{A_5}{8} \right] + \frac{GreA_{12}S}{72(1+2d)} + \frac{GreA_{13}S}{48(1+2d)} + \\
& + \frac{Gre Br S d (1+d)}{72(1+2d)} - \frac{GreS^2 d}{12(1+2d)} \left[\frac{A_4}{24} + \frac{A_5}{6} \right] - \frac{GreA_{12}S d (1+d)}{24(1+2d)} - \frac{GreA_{13}S d (1+d)}{12(1+2d)} + \\
& - \frac{Gre Br S d}{96(1+2d)} + \frac{GreS^2 d}{12(1+2d)} \left[\frac{A_4}{30} + \frac{A_5}{8} \right] + \frac{GreA_{12}S d}{36(1+2d)} + \frac{GreA_{13}S d}{24(1+2d)} - \frac{Gre^2 Br d}{(1+2d)} \left[\frac{A_4}{144} + \frac{A_5}{72} \right] - q
\end{aligned}$$

and

$$B = \frac{1}{12} + \frac{Gre Br}{144} - \frac{Gre Br}{144(1+2d)} - \frac{Gre Br d}{72(1+2d)}.$$

To know the values of mixed convection parameter Gre (critical values) at which the velocity of the fluid gives a negative value (reverse flow) at the plate $y = l$, then the critical values at $y = l$ are obtained from the turning point of the velocity, i.e. $\frac{du}{dy}\big|_{y=l} = 0$ while at $y = 0$ is not possible due to the moving nature of the plate. The critical values for different flow parameters are captured in Tab.2.

The skin friction τ expressed as coefficient of surface skin stress is given by

$$\tau_0 = \mu_1 \frac{du}{dy}\bigg|_{y=0},$$

$$\tau_l = \mu_2 \frac{du}{dy}\bigg|_{y=l}.$$

The rate of heat transfer expressed as local Nusselt number Nu at both plates is given by

$$Nu_0 = k_1 \frac{dT_f}{dy}\bigg|_{y=0},$$

$$Nu_l = k_2 \frac{dT_f}{dy}\bigg|_{y=l}.$$

4. Validation

By setting $Br = 0$, $\frac{dP}{dx} = 0$ and $d = 0$, the work of Jha and Ajibade has been recovered, see Tab.5.

5. Result and discussion

Viscous dissipation and wall conduction effects on a steady mixed convection Couette flow of heat generating/absorbing fluid moving in a vertical channel of some thickness d has been studied. The steady flow is governed by six basic parameters: that is Gre , which is mixed convection parameter, S heat

generating/absorbing parameter, Br Brinkman number, Pr Prandtl number, d the boundary thickness and q the constant mass flux. The value of Pr is chosen to be 0.71 throughout the work for air as the working fluid.

Figures 2 and 3 display the influence of Brinkman number Br on velocity and temperature. It can be seen that, velocity profile increases near the heated plate with increase in Br . This is true since, Brinkman number is the ratio of heat produced by viscous dissipation to heat transported by molecular conduction, therefore, the heat generated by viscous dissipation is higher than the external heating, which reduces the density of the fluid, hence increases the fluid flow and thermal boundary layer thickness. A reverse case was observed near the cold plate. This is because; the dissipation and wall conduction near the cold were low which increases the density of the fluid, hence retards the fluid flow. In Fig.3, the temperature profile increases with increase in Brinkman number. This is because; the heat generated by dissipation and wall conduction raises the temperature of the fluid. It is also observed that the inter-facial temperature grows on both surfaces due to the increase in dissipation heating.

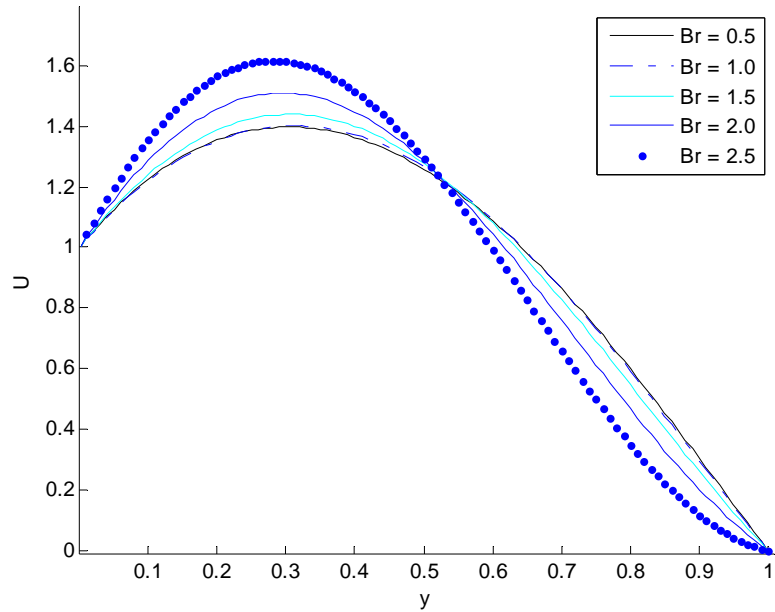


Fig.2. Velocity profile for different values of $Br(S = 0.4, Gre = 20, d = 0.2, q = 1)$.

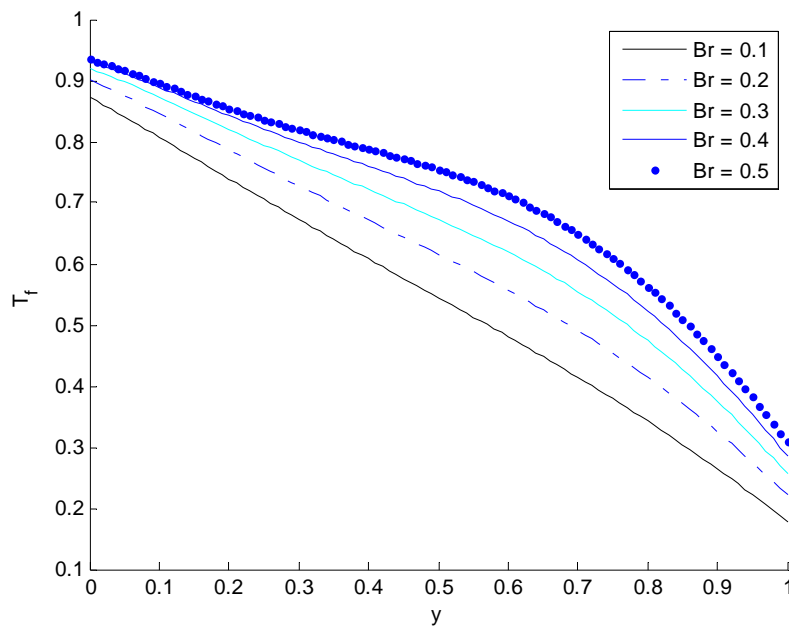


Fig.3. Fluid temperature profile for different values of $Br(S = 0.4, Gre = 20, d = 0.2, q = 1)$.

Figures 4 and 5 show the effect of heat generating/absorption parameter S on velocity and temperature profiles. The velocity profile increases near the heated plate with increase in heat generation $S < 0$. This is physically true since heat generated raises the fluid temperature which in turn reduces the density and increase the convection current of the fluid hence increases the fluid flow. However the fluid flow at the heated wall decreases with increase in heat absorption $S > 0$. This is physically true since the heat generated is absorbed by the fluid which makes the fluid dense, therefore reduces the temperature and slows down the fluid flow as well. The temperature profile increases with increase in heat generation $S < 0$, since the heat generated by wall conduction and dissipation increases the fluid temperature. On the other hand, the temperature profile decreases with increase in heat absorption $S > 0$. Furthermore the inter-facial temperature is more pronounced at the heated plate than the cold plate.

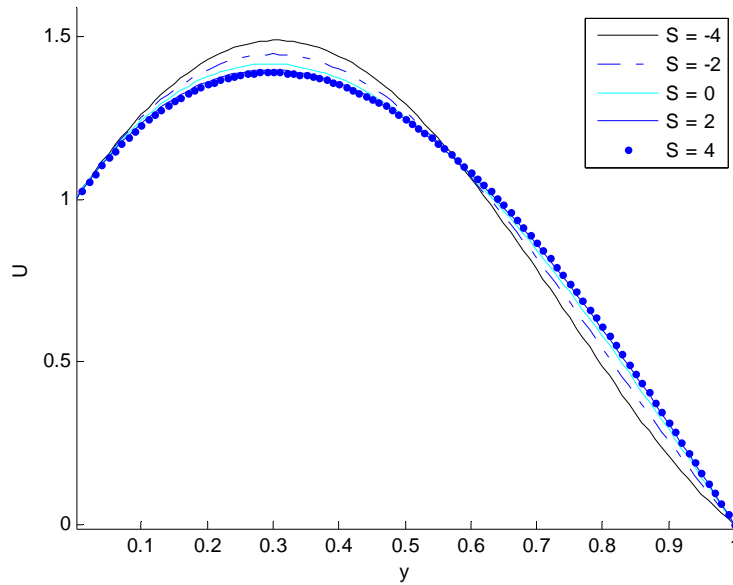


Fig.4. Velocity profile for different values of S ($Br = 0.2, Gre = 20, d = 0.2, q = 1$).

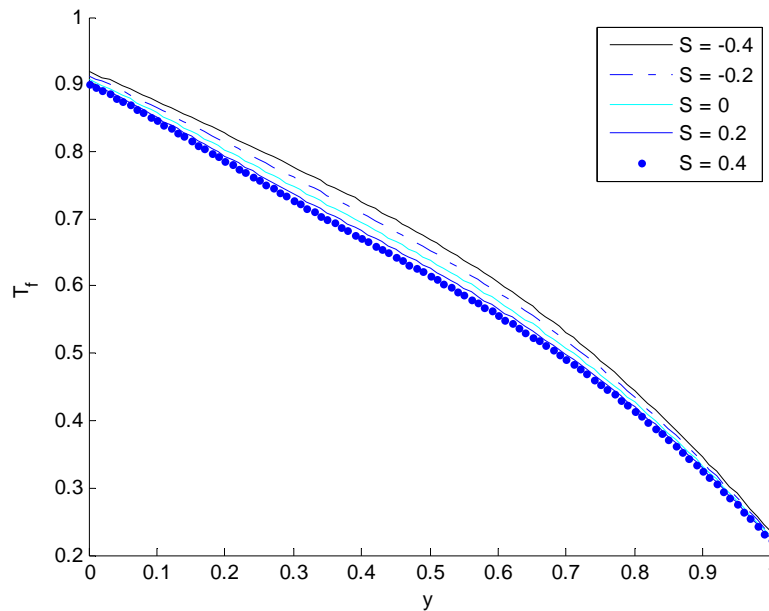


Fig.5. Fluid temperature profile for different values of S ($Br = 0.2, Gre = 20, d = 0.2, q = 1$).

The effect of mixed convection Gre is depicted on Figs 6 and 7 for velocity and temperature profiles respectively. The velocity profile increases with increase in Gre at the heated plate. This is true, when buoyancy forces dominate the viscous forces of the fluid, the velocity of the fluid increases, while near the cold plate a reverse case was observed. In Fig.7, the temperature profile at the heated plate increases with increase in mixed convection Gre . This is true, since the heat generated by wall conduction and dissipation is diffused by the buoyancy forces which in return increases the fluid temperature. Furthermore, the temperature profile decreases near the cold plate with increase in the thermal buoyancy forces. The effect of thermal buoyancy forces near the cold is so minimal and the inter-facial temperature is more influenced at the heated plate.

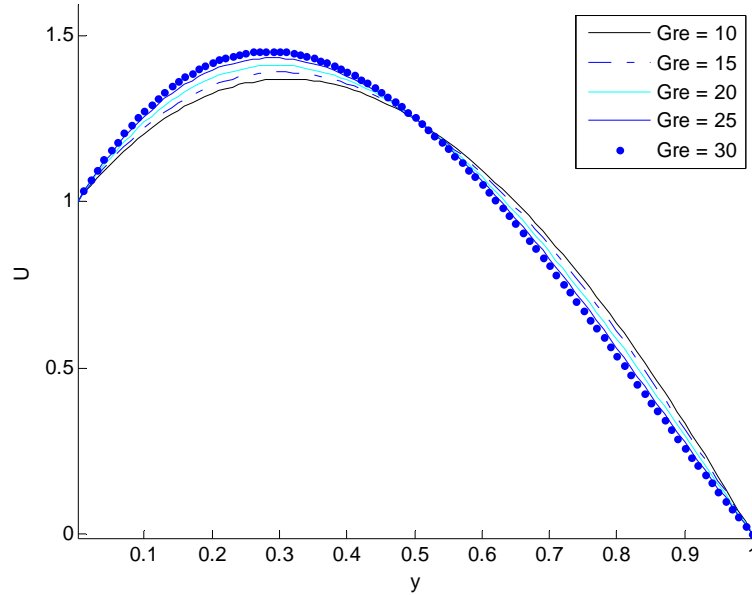


Fig.6. Velocity profile for different values of mixed convection parameter $Gre(Br = 0.2, S = 0.4, d = 0.2, q = 1)$.

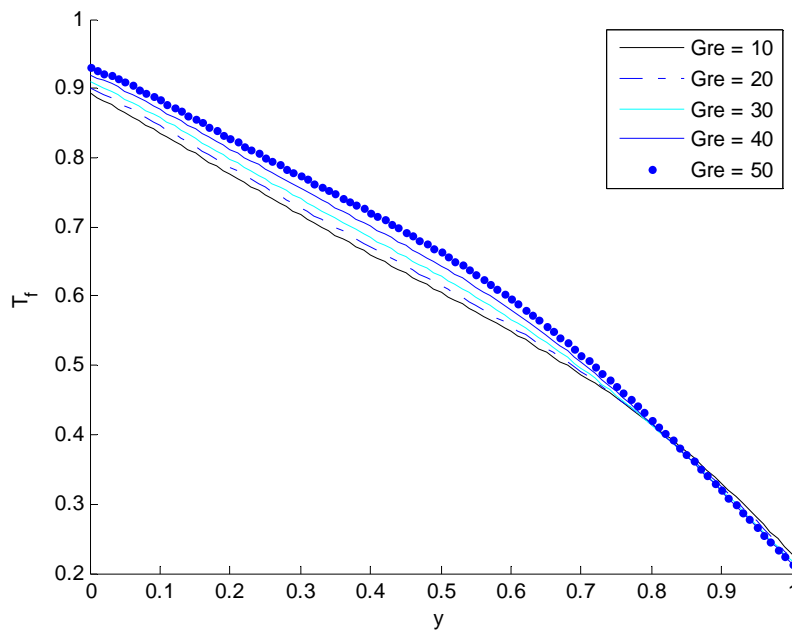


Fig.7. Fluid temperature profile for different values of mixed convection parameter $Gre(Br = 0.2, S = 0.4, d = 0.2, q = 1)$.

For different boundary layer thickness d , Figs 8 and 9 show the velocity and temperature profiles respectively. It can be seen from the graphs that, both the velocity and temperature profiles decrease near the heated plate with an increase in d . This is physically true since increase in the thickness of a material reduces the heat penetration through the system, which in return decreases the temperature as well as the velocity of the fluid. Toward the cold plate, the velocity and temperature profiles increase with increase in d . It is further observed that the inter-facial temperature is more affected by the boundary thickness at the cold plate.

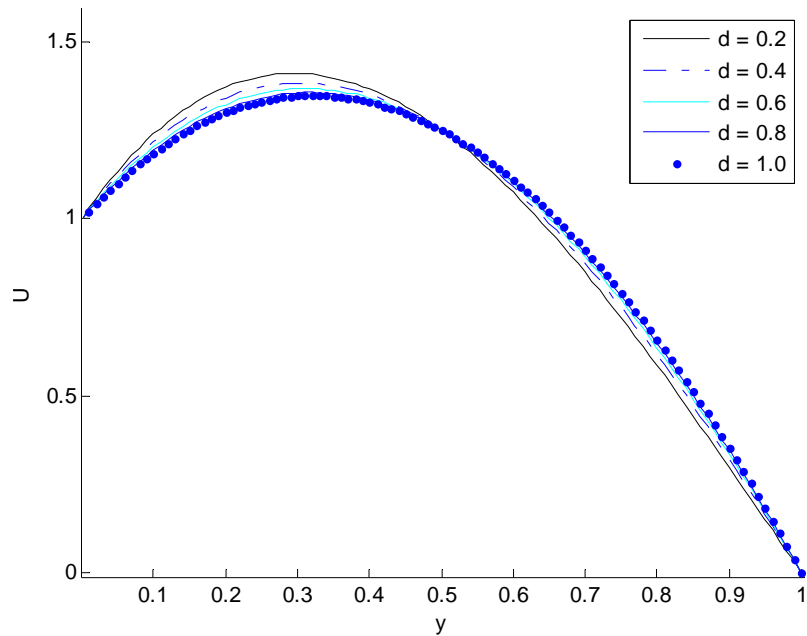


Fig.8. Velocity profile for different values of d ($Br = 0.2, S = 0.4, Gre = 20, q = 1$).

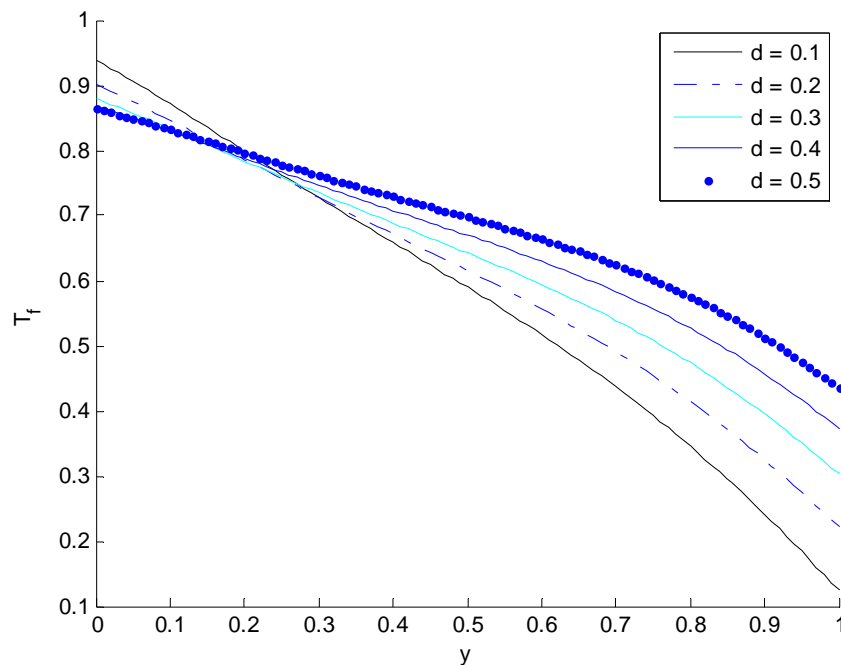


Fig.9. Fluid temperature profile for different values of d ($Br = 0.2, S = 0.4, Gre = 10, q = 1$).

Figures 10 and 11 display the velocity and temperature profiles for different values of constant mass flux q respectively. The velocity profile increases with increasing q . This is true since, increase in pressure gradient leads to increase in constant mass flux which eventually leads to increase in fluid flow. The temperature profile decreases with increase in q as shown in Fig.11.

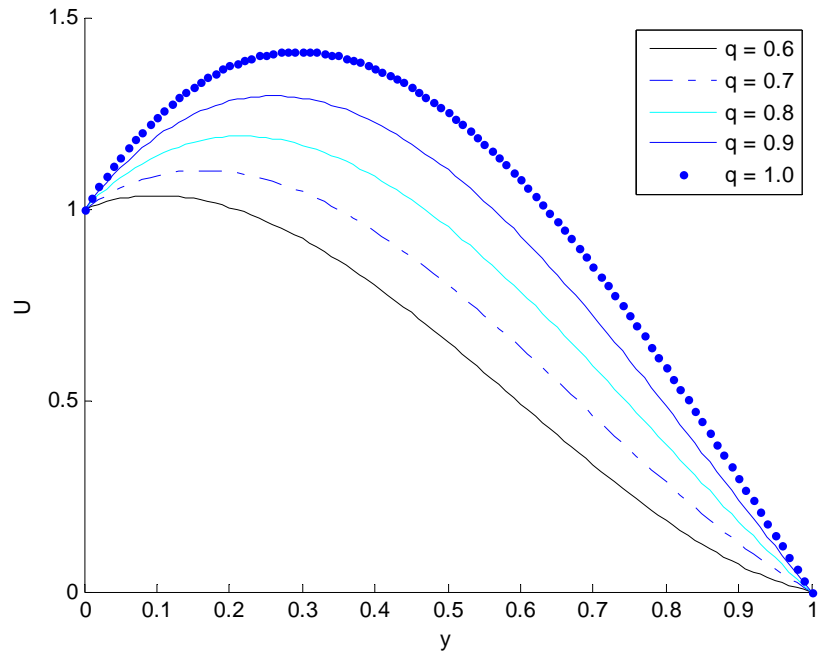


Fig.10. Velocity profile for different values of q ($Br = 0.2, S = 0.4, Gre = 20, d = 0.2$).

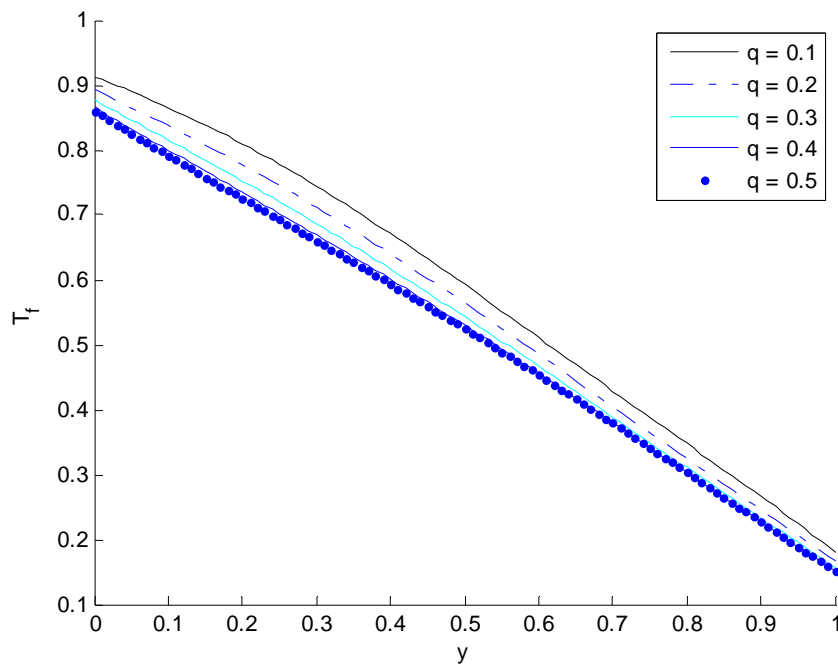


Fig.11. Fluid temperature profile for different values of q ($Br = 0.2, S = 0.4, Gre = 20, d = 0.2$).

Table 1 shows the variation of pressure gradient with the flow formation in the channel. It can be seen that, the pressure gradient increases with increase in mass flux q . An increase in mass flux requires an increase in pressure gradient to drive the flow. This is clearly obtained when Gre is relatively small. However, for large value of Gre in which natural convection dominance is pronounced, it requires a pressure gradient to act against the flow so as to maintain the desired flow mass flux, Hence the positive values of pressure at large Gre . The table further shows that, the pressure gradient required decreases when heat generation $S < 0$ increases. This is physically true since growing heat generation enhances the buoyancy and increase the natural convection so that with little contribution from the forced convection, the decreased mass flux is achieved.

Table 1. Variation of pressure gradient $\left(\frac{dP}{dx}\right)$ for different values of S , q , d and Gre where $Br = 0.2$.

S	q	$(d = 0.2, Gre = 10)$	$(d = 0.2, Gre = 20)$	$(d = 0.5, Gre = 20)$
		$\frac{dP}{dx}$	$\frac{dP}{dx}$	$\frac{dP}{dx}$
-0.4	1	-0.0875	5.9271	7.3219
-0.2		-0.3259	5.4502	6.3850
0		-0.5490	5.0041	5.5429
0.2		-0.7567	4.5887	4.7955
0.4		-0.9490	4.2041	4.1429
-0.4	2	-12.0875	-6.0729	-4.6781
-0.2		-12.3259	-6.5498	-5.6150
0		-12.5490	-6.9959	-6.4571
0.2		-12.7567	-7.4113	-7.2045
0.4		-12.9490	-7.7959	-7.8571

Table 2 shows the critical values of Gre at the cold plate $y = 1$. It can be observed from the table that, smaller critical values can be obtained by enhancing the viscous dissipation parameter Br or the heat generation parameter $S < 0$. This is so because as the viscous dissipation or heat generation increases, the convection current of the fluid increases hence, it requires a lower value of the mixed convection parameter to nullify the boundary friction on the plate. However, increasing the boundary plate thickness, mass flux and heat absorption raise the critical value of Gre . This is in line with the fact that, fluid temperature decreases thereby weakening the convection current so that an increased Gre is required to nullify the boundary friction. A general view of this table indicates that, each phenomenon that boosts convection current requires a decrease in Gre while the reverse case is observed for each activity that weakens the convection current.

Table 2. Critical values of Gre at the stationary plate $y = 1$ for different values of the flow parameters.

S	Br	$(d = 0.2, q = 1)$	$(d = 0.2, q = 2)$	$(d = 0.5, q = 2)$
		Gre_1	Gre_1	Gre_1
-0.4	0.2	58.4196	133.1999	137.6610
-0.2		60.9293	139.8852	152.8247
0		63.5794	146.9752	170.7078
0.2		66.3715	154.4536	191.5662
0.4		69.3040	162.2847	215.2908
-0.4	0.4	50.1215	104.4946	97.36120
-0.2		52.3964	109.1904	106.4693
0		54.8072	114.0664	116.7303
0.2		57.3546	119.0935	128.1226
0.4		60.0352	124.2328	140.4834

Table 3 displays the shear stress τ between the fluid and the plates. It is observed that, the skin friction increases at the heated with increase in mixed convection while it decreases with increase in boundary plate thickness. Increase in mixed convection Gre leads to a decrease in skin friction while it increases with increase in boundary plate thickness d . On the other hand, when heat generation $S < 0$ is increased, there is an increase in skin friction at the heated and cold plates while it decreases with an increase in heat absorption $S > 0$.

Table 3. Skin friction τ at the heated plate $y=0$ and the cold plate $y=1$, for different values of S , d and Gre where $Br=0.2$ and $q=1$.

S	$(d=0.2, Gre=10)$		$(d=0.2, Gre=20)$		$(d=0.5, Gre=20)$	
	τ_0	τ_1	τ_0	τ_1	τ_0	τ_1
-0.4	2.4946	3.1844	3.0053	2.8722	2.6570	3.4347
-0.2	2.4965	3.1827	3.0027	2.8356	2.6331	3.3477
0	2.4980	3.1814	2.9997	2.8017	2.6108	3.2702
0.2	2.4991	3.1803	2.9963	2.7766	2.5900	3.2021
0.4	2.4998	3.1796	2.9925	2.7422	2.5707	3.1436

The rate of heat transfer Nu has been captured in Tab.4. It shows that, the rate of heat transfer at the heated plate decreases with increase in heat generation $S < 0$ while it increases at the cold plate except in the cases when the boundary plate thickness is increased to 0.5 . Increase in dissipating parameter Br leads to a decrease in heat transfer at the heated plate while it increases at the cold plate for relatively small heat generation $S < 0$. Decrease in heat transfer at the heated and increase in heat transfer at the cold plates is attributed to induced buoyancy of the hydrodynamic and thermal strength of the fluid brought about by the actions of growth in shear stress which leads to an increase in temperature difference near the cold plate and a reduction near the heated plate. It's further observed when the boundary plate thickness is increased, the rate of heat transfer on both the channel plates (heated and cold) decreases.

Table 4. Rate of heat transfer Nu at the heated plate $y=0$ and the cold plate $y=1$, for different values of S , d and Br where $Gre=10$ and $q=1$.

S	$(d=0.2, Br=0.2)$		$(d=0.2, Br=0.5)$		$(d=0.5, Br=0.5)$	
	Nu_0	Nu_1	Nu_0	Nu_1	Nu_0	Nu_1
-0.4	0.3709	1.1646	0.1883	1.5641	0.0882	1.2181
-0.2	0.4181	1.1322	0.2132	1.5526	0.1013	1.2194
0	0.4608	1.1031	0.2325	1.5445	0.0980	1.2326
0.2	0.4997	1.0769	0.2471	1.5390	0.0827	1.2534
0.4	0.5354	1.0528	0.2579	1.5351	0.0593	1.2780

6. Conclusion

The present work studied effect of wall conduction on a steady mixed convection flow in the presence of viscous dissipation and boundary layer thickness. The work concluded that, the velocity profile increases near the heated plate with increase in Br and Gre while it decreases towards the cold plate with increase in Br and Gre . Moreover, the velocity profile decreases near the heated plate with increase in heat absorption $S > 0$ and d and reverse cases were observed toward the cold plate. It is concluded that, the temperature profile increases with increase in Br and heat generation parameter $S < 0$ while it decreases with increase in heat absorption $S > 0$ and constant mass flux q . The inter-facial temperature is affected by the

governing flow parameters. It is further observed that the rate of heat transfers on heated and cold plates decrease with increasing boundary plate thickness d . Likewise, the shear stress decreases on the heated plate with growing d and increases at the cold plate with increase in d . It is further concluded that, smaller critical values can be obtained by enhancing the viscous dissipation Br . When suppressing Brinkman number, pressure gradient and boundary plate thickness, i.e ($Br = 0, \frac{dP}{dx} = 0$ and $d = 0$), the work of Jha and Ajibade [17] is recovered, (see Tab.5).

Table 5. Comparison of the present work and Jha and Ajibade (2010).

S	Jha and Ajibade (2010) $Gr = 10, y = 0.5$		Present Work $Gr = 10, y = 0.5, Br = 0, d = 0, \frac{dp}{dx} = 0$	
	Velocity	Temperature	Velocity	Temperature
1	1.065905580149630	0.443409441985037	1.066514756944445	0.443348524305556
0.5	1.094022828643205	0.470298858567840	1.094102647569445	0.470294867621528
-0.5	1.159295152484090	0.532964757624204	1.159206814236111	0.532960340711806
-1	1.197469636622746	0.569746963662275	1.196723090277778	0.569672309027778

Nomenclature

- Br – Brinkman number
- d – boundary plate thickness (L)
- Ec – Eckert number
- Gre – mixed convection parameter
- g – acceleration due gravity (ms^{-2})
- k – thermal conductivity of the fluid ($Wm^{-1}k^{-1}$)
- k_1 – thermal conductivity of the plate p_1 ($Wm^{-1}k^{-1}$)
- k_2 – thermal conductivity of the plate p_2 ($Wm^{-1}k^{-1}$)
- kr_1 – thermal conductivity ratio between the fluid and plate p_1
- kr_2 – thermal conductivity ratio between the fluid and plate p_2
- P – pressure of the fluid (Pa)
- Pr – Prandtl number
- p_1 – channel plate 1
- p_2 – channel plate 1
- Q_0 – heat generation/absorption coefficient
- T_f – temperature of the fluid (K)
- T_{p_1} – temperature of the plate p_1 (K)
- T_{p_2} – temperature of the plate p_2 (K)
- T_w – temperature of the heated wall (K)
- T_0 – temperature of the cold wall (K)
- u – velocity of the fluid (ms^{-1})
- x – distance along y -direction
- y – distance along x -direction
- α_1 – thermal diffusivity of the plate p_1 (m^2s^{-1})

- α_2 – thermal diffusivity of the plate p_2 ($m^2 s^{-1}$)
 β – thermal expansion coefficient (k^{-1})
 ν – kinematic viscosity ($m^2 s^{-1}$)
 ρ – fluid density ($kg m^{-3}$)

References

- [1] Kevin D.C. and Barbaros C. (2011): *The effects of axial conduction on heat transfer in a liquid microchannel flow.* – International Journal of Heat and Mass Transfer, vol.54, No.11-12, pp.2542-2549.
- [2] Michael J.S. and Dimos P. (2005): *Effect of microreactor wall conduction on the reforming process of methane.* – Chemical Engineering Science, vol.60, pp.6983-6997
- [3] Hassab M.A., Khamis M.M. and Shawky I.M. (2013): *The effect of axial wall conduction on heat transfer parameters for a parallel-plate channel having a step change boundary conditions.* – Numerical Heat Transfer: Part A, vol.63, pp.430-451.
- [4] Ates A., Darici S. and Bilir S. (2007): *Transient conjugated heat transfer in thick walled pipes with uniform heat flux boundary conditions.* – 5th International Conference on Heat Transfer, Fluid Mechanics and Thermodynamics, HEFAT.
- [5] Mei L., Wang Q.W. and Zhixiong G. (2016): *Investigation on evaluation criteria of axial wall heat conduction under two classical thermal boundary conditions.* – Applied Energy, vol.162, pp.1662-1669.
- [6] Moukalled F., Darwish M. and Acharya S. (1995): *Influence of wall conduction on mixed convection heat transfer in externally finned pipes.* – Numerical Heat Transfer, Part A: Application, vol.28, No.2, pp.157-173.
- [7] Hamid N. and Behnam R. (2012): *Mixed convective slip in a vertical plate microchannel with symmetric and asymmetric wall heat fluxes.* – Transaction of the Canadian Society for Mechanical Engineering, vol.36, No.3, pp.207-218.
- [8] Ajibade O.A. and Thomas U.O. (2017): *Entropy generation and irreversibility analysis due to steady mixed convection flow in a vertical porous channel.* – International Journal of Heat and Technology, vol.35, No.3, pp.433-446.
- [9] Swati M. (2012): *Mixed convection boundary layer flow along a stretching cylinder in porous medium.* – Journal of Petroleum Science and Engineering, vol.76-97, pp.73-78.
- [10] Jha K.B., Debora D. and Ajibade O.A. (2015): *Mixed convection in an inclined channel filled with porous material having time periodic boundary conditions.* – Transport in Porous Media, vol.109, No.1, DOI 10.1007/s11242-015-0533-6.
- [11] Mehdi M. and Mohsen S. (2015): *MHD mixed convection slip flow in a vertical parallel plate microchannel heated at asymmetric and uniform heat flux.* – Journal of Mechanical Science and Technology, vol.29, No.7, pp.1-8.
- [12] Jha K.B., Debora D. and Ajibade O.A. (2013): *Steady fully developed mixed convection flow in a vertical parallel plate microchannel with bilateral heating and filled with porous material.* – Journal of Process Mechanical Engineering, vol.227, No.1, pp.56-66.
- [13] Jha K.B. and Babatunde A. (2014): *Mathematical modeling and exact solution of steady fully developed mixed convection flow in a vertical micro-porous-annulus.* – Afrika Matematika, DOI 10.1007/s13370-014-0277-4.
- [14] Dileep S.C. and Vikas K. (2011): *Radiation effects on mixed convection ow and viscous heating in a vertical partially filled with a porous medium.* – Tankang Journal of Science and Engineering, vol.14, No.2, pp.97-106.
- [15] Joseph K.M., Peter A. and Abubakar S.M. (2017): *Effect of Brinkman number and magnetic field on Laminar convection in a vertical plate channel.* – Science World Journal, vol.12, No.4, pp.58-62.

- [16] Pranab K.M. and Sanchayan M. *Viscous dissipation effects on the limiting value of Nusselt numbers for a shear driven flow between two asymmetrically heated parallel plates.* – *Frontiers in Heat and Mass Transfer*, 3(033004), (212).
- [17] Jha K.B. and Ajibade O.A. (2010): *Unsteady free convective Couette flow of heat generating/absorbing fluid.* – *International Journal of Energy and Technology*, vol.2, No.12, pp.1-9.
- [18] Jha B.K., Michael O.O. and Babatunde A. (2016): *Steady fully developed mixed convection flow in a vertical micro-concentric annulus with heat generating/absorbing fluid: an exact solution.* – *Ain Shams Engineering Journal*, DOI.org/10.1016/j.asej.2016.08.005.
- [19] Vajravelu K. and Sastri K.S. (1978): *Laminar free convection heat transfer of a viscous in-compressible heat generating fluid flow past a vertical porous plate in the presence of free-stream oscillations I.* – *Acta Mechanica*, vol.31, pp.71-87.
- [20] Vajravelu K. and Sastri K.S. (1978): *Laminar free convection heat transfer of a viscous incompressible heat generating fluid flow past a vertical porous plate in the presence of free-stream oscillations II.* – *Acta Mechanica*, vol.31, pp.80-100.
- [21] Vajravelu K. (1979): *Natural convection at a heated semi infinite vertical plate with temperature dependent heat sources or sinks.* – *Proceeding of the Indian Academy of Sciences*, vol.88, No.4, pp.369-376.
- [22] Moalem D. (1976): *Steady-state heat transfer within porous medium with temperature dependent heat generation.* – *International Journal of Heat and Mass Transfer*, vol.19, pp.529-537.
- [23] Foraboschi F.P. and Federico I.Di. (1964): *Heat transfer in Laminar flow of non-Newtonian heat generating fluids.* – *International Journal of Heat and Mass Transfer*, vol.7, No.3, pp.315-318.
- [24] Jafar B. and Hossein A. (2009): *Study of convergence of Homotopy Perturbation Method for systems of partial differential equations.* – *Computer and Mathematics with Application*, vol.58, pp.2221-2230.
- [25] Asma A.E., Adem K. and Bachok M.T. (2014): *Note on the convergence analysis of Homotopy Perturbation Method for fractional partial differential equations.* – *Abstract and Analysis*, ID803902:8 pages.
- [26] Elsayed A.M.A., Elkalla I.L. and Hammad D. (2012): *A homotopy perturbation technique for solving partial differential equations of fractional order in infinite domains.* – *Applied Mathematics and Computation*, pp.8329-8340.
- [27] Jafar H., Alipour A. and Tajadodi H. (2012): *Convergence of homotopy perturbation method for solving integral equations.* – *Thai Journal of Mathematics*, vol.8, No.3, pp.511-520.
- [28] He J.H. (1999): *Homotopy perturbation technique.* – *Computer Methods in Applied Mechanics and Engineering*, vol.178, pp.257-262.
- [29] He J.H. (2000): *A coupling method of a homotopy perturbation technique for non-linear problems.* – *Journal of Non-Linear Mechanics*, vol.35, pp.37-43.
- [30] He J.H. (2003): *Homotopy perturbation method: a new nonlinear analytical technique.* – *Applied Mathematics and Computation*, vol.135, pp.73-79.
- [31] He J.H. (2006): *Homotopy perturbation method for solving boundary value problems.* – *Physics Letters A*, vol.350, pp.87-88.

Received: December 7, 2018

Revised: July 21, 2019